Prostate Imaging

4

Axel Wetter and Matthias Eiber

4.1 Prostate Cancer: Epidemiology and Pathology

In developed countries, prostate cancer is one of the most common malignancies with an incidence of 69.5 cases per 100,000 men, and is considered to be among the five leading causes of death worldwide (Torre et al. 2015). In 95% of all malignant prostate tumors, prostate cancer arises from acinar epithelial cells and is therefore defined as an adenocarinoma. Rare entities of prostate cancer include neuroendocrine or sarcomatoid prostate cancers. Pathological and clinical staging of prostate cancer is based on the TNM classification, providing information about the primary tumor (T-stage), lymph node metastases (N-stage) and distant metastases (M-stage). T1 defines a clinically inapparent tumor (not detectable by imaging), T2 a tumor confined to the gland, T3 a tumor with extracapsular growth and T4 a tumor that infiltrates adjacent tissue (TNM classification of malignant tumors, eighth edition). Grading of prostate cancer is almost exclusively based on the Gleason grading system (Gleason grading), whereby the tumor is described by an increasing loss of differentiation, displayed in Gleason patterns from 1 to 5. As there are often several growth patterns within the prostate, the most common and second most common Gleason pattern is recorded and reported as the Gleason sum score, ranging from 2 to 10 (Gleason 1966). Staging and grading of prostate cancer are of utmost importance for further therapy decisions. From a clinical point of view, the information derived from staging, grading and other variables, such as the PSA value, are used for outcome prediction and are implemented in nomograms such as the Partin tables (Partin et al. 1993).

4.2 Prostate Cancer: MR Imaging

MR imaging of the prostate has become the leading imaging modality for tumor detection and local staging of prostate cancer. Due to its high soft tissue contrast, MRI enables detailed visualization of the zonal anatomy of the prostate, including differentiation of the central, peripheral and transition zone, anterior fibomuscular stroma, periurethral region and seminal vesicles. Morphological MR imaging of the prostate is primarily based on high-resolution strong T2-weighted fast-spin-echo images, where the healthy peripheral zone and the seminal vesicles exhibit a hyper-intense signal, whereas the transi-

A. Wetter, M.D. (✉)
Department of Diagnostic and Interventional Radiology and Neuroradiology, University Hospital Essen, Essen, Germany
e-mail: axel.wetter@uk-essen.de

M. Eiber, M.D.
Department of Nuclear Medicine, Technical University Munich, Munich, Germany

L. Umutlu, K. Herrmann (eds.), *PET/MR Imaging: Current and Emerging Applications*,
https://doi.org/10.1007/978-3-319-69641-6_4

tional zone exhibits a hypo-intense signal. Over the past years, MR imaging of prostate cancer has emerged from sole morphological imaging to a multiparametric imaging approach, combining anatomical and functional data by the implementation of diffusion-weighted imaging (DWI) and dynamic contrast-enhanced imaging (DCE) (Hricak et al. 1983, Fütterer et al. 2006, Morgan et al. 2007). DWI in prostate cancer is based on the presumption that high cellularity leads to decreased movement of water molecules which are insensitive for the so-called diffusion sensitizing gradients, hence resulting in retention of their high signal despite increasing diffusion sensitizing gradients. DCE is based on the assumption that prostate cancer lesions display a focal and early enhancement due to pathological tumor vessels. Numerous studies have shown that the combined analysis of morphological and functional MR-datasets leads to significantly improved detection of prostate cancer foci (Hamoen et al. 2015). The European Society of Urogenital Radiology (ESUR) and the American College of Radiologists (ACR) have made efforts to standardize mpMRI of the prostate and have proposed a standardized approach, the Prostate Imaging Reporting and Data System (PI-RADS) for lesion characterization (Barentz et al. 2012, Weinreb et al. 2016). In its newest version (PI-RADSv2), PI-RADS is based on T2-weighted imaging, DWI and DCE. Suspicious prostate lesions are graded using both a score from 1 to 5 in T2-weighted images and DWI, whereby DWI is the dominant sequence for lesion detection of the peripheral zone, and T2-weighted imaging is dominant for lesion characterization of the transitional zone. DCE is assessed on the existence or absence of pathological early enhancement and may lead to an upgrade of a PI-RADS score 3-lesion in the peripheral zone to a score of 4. Minimum field strength of 1.5 T is recommended, but preference is given to 3 T scanners. According to PI-RADS v2, use of an endorectal coil is not necessary at 3 T, but might be useful in 1.5 T scanners in order to improve signal-to-noise ratio. Typical prostate cancer lesions are strongly hypointense in T2-weighted images and display a diffusion restriction with a high signal in the original diffusion-weighted images and a concomitant signal drop in the ADC maps. DCE typically demonstrates a focal and earlier enhancement than corresponding areas of non-malignant prostate tissue. Sufficient diagnostic accuracy for the detection of prostate cancer has been shown when using PI-RADS (Hamoen et al. 2015). Table 4.1 illustrates a typical MR sequence protocol for prostate, pelvic and whole-body MR imaging as part of a PET/MRI protocol.

Table 4.1 Set of MR-sequences combining the application of multi-parametric prostate MRI, pelvic MRI and whole-body MRI within a hybrid PET/MR examination

Sequence	TR (ms)	TE (ms)	FoV (mm)	Slice thickness (mm)	Matrix	*B*-values (s/mm²)
TIRM coronal pelvis	3110	56	380	5	273 × 448	
T2 FSE axial pelvis	4311	114	400	7	512	
T2 FSE axial prostate	4360	101	200	3	310 × 320	
T2 FSE coronal prostate	4000	101	200	3	310 × 320	
T2 FSE sagittal prostate	3740	101	200	3	310 × 320	
DWI prostate	7600	89	260	3	102 × 160	0, 1000, 1500, 2000
DWI pelvis	8100	70	420	5	90 × 160	0, 500, 1000
T1 vibe axial pre flip 2 deg. nativ prostate	4.24	1.31	300	3	114 × 192	
T1 vibe axial pre flip 15 deg. nativ prostate	4.24	1.31	300	3	114 × 192	
T1 vibe axial dyn prostate (DCE)	4.24	1.31	300	3	114 × 192	
T1 FSE axial 5 mm fs pelvis	606	10	400	5	176 × 512	
T1 vibe dixon axial contrast wholebody	4.05	1.29	380	3.5	173 × 320	

4.3 Prostate Cancer: PET and PET/CT Imaging

While MR imaging characterizes prostate lesions on the basis of morphological and functional data, PET imaging adds information on metabolism or target expression, depending on the specific tracer used. At present, two types of radiopharmaceuticals for PET imaging of prostate cancer are employed: choline derivatives or small molecules targeting the prostate-specific membrane antigen (PSMA). The employment of choline tracers is based on the observation that prostate cancer harbors an increased uptake of choline as a precursor for the synthesis of phosphorylcholine and ultimately phosphatidylcholine in tumor cells. Carbon-11-choline was originally introduced for PET imaging of brain tumors, but was later also utilized for prostate cancer imaging (Hara et al. 1998). The development of ^{18}F labeled choline derivatives such as ^{18}F fluoroethylcholine had the advantage of a markedly longer half-life period and shorter positron range (Hara et al. 2002). More recently, PSMA ligands have moved into the focus of prostate cancer imaging. PSMA is a transmembrane glycoprotein and functions as a cell surface peptidase (Sweat et al. 1998). It is highly over expressed (100–1000 fold) on almost all prostate cancer cells and most of its metastases, making it a highly valuable target for prostate cancer imaging. In this coherence, a ^{68}Ga labeled PSMA ligand (Glu-NH-CO-NH-Lys-(Ahx)-^{68}Ga-HBED-CC, ^{68}Ga PSMA-HEBD-CC or ^{68}Ga PSMA-11) was successfully introduced in 2012 and is the most commonly used PSMA ligand to date (Afshar-Oromieh et al. 2013). Most recently, ^{18}F-PSMA 1007, an ^{18}F labeled PSMA ligand has been developed, combining the high specificity of PSMA with reduced urinary clearance, hence reducing the diagnostically challenging "halo"-effect (caused by tracer accumulation in the bladder and consecutive overlapping uptake) (Giesel et al. 2017).

So far, main indications for PET and PET/CT imaging with radiolabeled choline focus on patients with biochemical recurrence after radical prostatectomy or radiation therapy and on patients with high-risk prostate cancer for initial staging. Emerging indications are stratifications into different therapeutic groups (e.g., eligibility for salvage lymphadenectomy) and prediction of the patient's prostate cancer-specific survival (Giovacchini et al. 2017). In recent years, PET/CT imaging with ^{68}Ga PSMA-11 has been extensively investigated and has shown high clinical value in prostate cancer imaging. It has proven to be superior over choline derivatives in terms of lesion detection, lesion-background contrast and tracer uptake in recurrent prostate cancer. Especially in early recurrent disease (e.g. PSA < 1 ng/ml) ^{68}Ga PSMA-11 has demonstrated the ability to successfully detect tumor lesions which are usually occult in other imaging modalities, including ^{18}F-Choline-PET/CT imaging (Afshar-Oromieh 2016).

4.4 Prostate Cancer: PET/MR Imaging

Integrated PET/MR imaging is based on the integration of a PET scanner into an MR scanner in order to enable simultaneous data acquisition with both modalities during one session. Simultaneous scanning without the necessity of moving the patient from one scanner to another enables excellent co-registration of suspicious lesions (even of lesions of smaller size), which is known to be hampered in sequentially fused hybrid imaging. Furthermore, the addition of excellent soft-tissue contrast and the possibility to combine functional information from MRI (DWI, DCE) with molecular information from PET holds promise of increasing the diagnostic capability. From a technical point of view, simultaneous PET/MR scanning is demanding, as several preconditions—from structural integration of both scanners to deployment of specific hardware such as receiver coils and novel PET detector crystals, as well as specific requirements such as different techniques for scatter and attenuation correction—have to be met in order to provide a well-performing employment in clinical routine. Since the first preclinical scan with an integrated PET/MR

scanner in 2008 (Pichler et al. 2008), numerous studies have been carried out in order to investigate this new technology in the field of prostate cancer.

4.4.1 Technical Evaluation and Feasibility

Over the past few years, simultaneous PET/MRI has proven to be a robust method under clinical conditions. PET images derived from PET/MRI have been shown to provide the same image quality as PET images derived from PET/CT; however, certain differences in quantitative values (e.g. SUVs) calculated from both modalities can be observed for a variety of reasons, such as MR-based attenuation correction, novel image reconstruction algorithms as well as the timing and length of the PET acquisition (Drzezga et al. 2012, Souvatzoglou et al. 2013, Wetter et al. 2014). Therefore, quantification of PET data derived from PET/MR remains challenging, and bone lesions in particular require careful attention, as underestimation of tracer uptake is frequently observed (Seith et al. 2016). The possibility of combining multiparametric prostate MRI with the PET scan draws particular attendance to investigate primary prostate cancer with integrated PET/MRI. The feasibility of simultaneous PET/MRI in primary prostate cancer was demonstrated shortly after the launch of commercially available integrated PET/MR scanners in 2013 (Wetter et al. 2013).

As PET imaging of prostate cancer with ^{68}Ga PSMA-11 is regarded to be superior to choline derivatives, employing and evaluating this technique using hybrid PET/MR is of utmost promise. An initial report on the application of ^{68}Ga PSMA-11 PET/MRI demonstrated its technical feasibility (Afshar-Oromieh 2014). Drawbacks of ^{68}Ga PSMA-11 PET/MRI are "halo" artifacts around the urinary bladder and kidneys which are supposed to result from inaccurate scatter correction especially in regions with high tracer uptake. Apart from continuous work and improvement on reconstruction algorithms, a practical work-around for this challenge is forced diuresis, which reduces the tracer concentration in the urinary bladder and consequently also reduces the halo effect. The recent introduction of ^{18}F PSMA-1007 might overcome this problem as it has only minimal urinary excretion (Giesel et al. 2017).

4.4.2 Clinical Workflow and Protocols

Initial investigations on PET/MRI put the focus on clinical workflow as well as protocols for whole-body fully integrated PET/MR imaging for different oncological tumor entities including prostate cancer (Martinez-Moeller et al. 2012, Souvatzoglou et al. 2013). These considerations were driven by the fact that compared with PET/CT, PET/MRI is a complex technique resulting in new problems and challenges, especially regarding workflow, scan protocols, and data analysis. This complexity applies in particular to examinations in oncology with partial- or whole-body coverage extending over several bed positions. Unlike diagnostic PET/CT, for which the clinical CT protocols can largely be copied from stand-alone CT, the design of a diagnostic MRI protocol for partial- or whole-body coverage is more complex and has to be adapted to the special requirements of PET/MRI to be both time-efficient and comprehensive.

4.5 Diagnostic Performance

4.5.1 Primary Prostate Cancer

Initial studies investigated the use of choline derivatives in PET/MR. Advantages compared to PET/CT arise from the potential of improved discrimination between malignant lesions and areas of benign prostatic hyperplasia which may exhibit similar choline uptake in PET but show different characteristics on MR. Recent studies using PET/MRI in primary prostate cancer described a higher diagnostic capability in terms of sensitivity and positive predictive value for tumor lesion detection compared to multiparametric MRI alone (Lee et al. 2017, Piert et al. 2016). This is regarded to result from the complimentary information of PET and functional MRI combined with exact matching of the PET data and MRI data in suspicious lesion.

Using ^{68}Ga PSMA-11 PET/MRI, preliminary results indicate that it might be at least equivalent to standalone multiparametric MRI for intraprostatic tumor localization (Eiber et al. 2015). Exploiting combined ^{68}Ga-PSMA11 PET/MRI for direct comparison in 53 intermediate/high risk patients the sensitivity of mpMRI using PI-RADS criteria amounted to 43% compared to 64% for ^{68}Ga-PSMA11 PET. Simultaneous PET/MRI, combining functional and mpMR data, further improved sensitivity to 76%. When compared to published data for mpMRI, ^{68}Ga PSMA-11 PET/MRI shows comparable sensitivity but notably higher specificity (Eiber et al. 2015). Important application areas of ^{68}Ga PSMA-11 PET/MRI may include precise radiation therapy planning or biopsy targeting with PET/MRI-based, ultrasound-guided or in-bore biopsy systems in order to use the improved tumor detection ability of ^{68}Ga PSMA-11 PET/MRI in patients with previously negative prostate biopsies. Figure 4.1 gives an example of a multi-

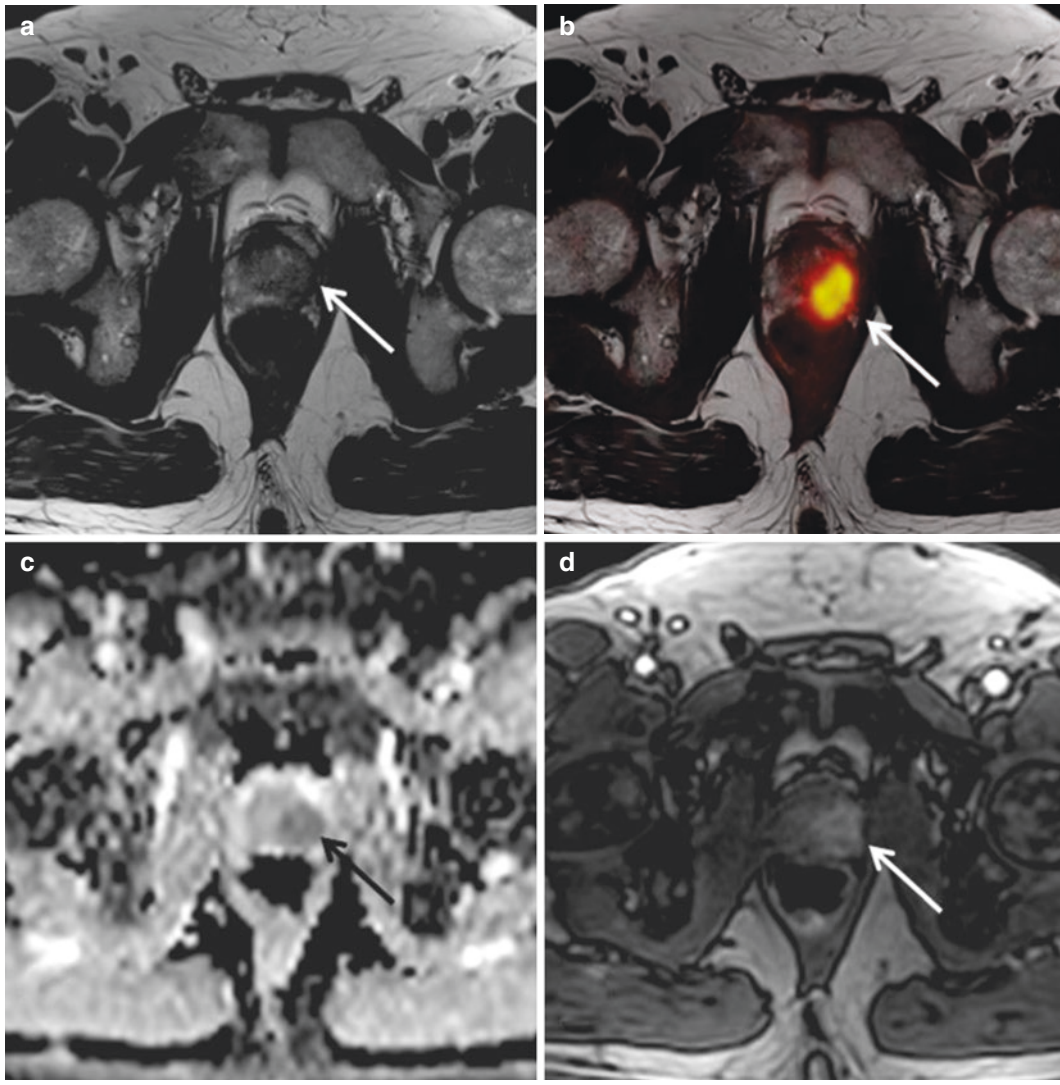

Fig. 4.1 ^{68}Ga PSMA-11 PET/MR images from a patient with biopsy-proven Gleason 4 + 4 prostate cancer at initial staging. The images demonstrate exemplarily the combination of multi-parametric MRI with PET. The prostate harbors a large hypo-intense lesion of the left peripheral and parts of the transitional zone (**a**) with increased ^{68}Ga PSMA-11 uptake (**b**), diffusion restriction, shown as a corresponding hypo-intensity in the ADC map (**c**), and pathological early enhancement in dynamic-contrast-enhanced imaging (**d**)

parametric MR examination combined with PET in a patient with a biopsy-proven prostate carcinoma.

4.5.2 Recurrent Prostate Cancer

Imaging of biochemical recurrence of prostate cancer is probably the most important field of PET imaging with choline derivatives or PSMA ligands. Especially precise imaging of the prostate bed after radical prostatectomy is challenging, as this anatomical region is complex due to scar tissue and postoperative changes as well as urine collection at the urethro-urethral anastomosis. As a result of this, both MR imaging and PET imaging are limited on their own, as scar tissue might be misinterpreted as local recurrence in MRI, and a potential local recurrence might be overlooked in PET/CT due to limited soft tissue contrast. In this regard, integrated PET/MRI offers a solution, as unclear tracer accumulations in the prostate bed can be precisely assigned to anatomical structures and suspicious soft-tissue lesions. Moreover, the multiparametric approach including diffusion-weighted imaging and contrast-enhanced imaging allows for improved characterization of unclear PET positive lesions in the prostate bed (Lütje et al. 2017, Freitag et al. 2017). Figures 4.2 and 4.3 outline the additional value of mpMRI to PSMA-ligand PET and choline PET by using PET/MRI in patients with biochemical recurrent prostate cancer.

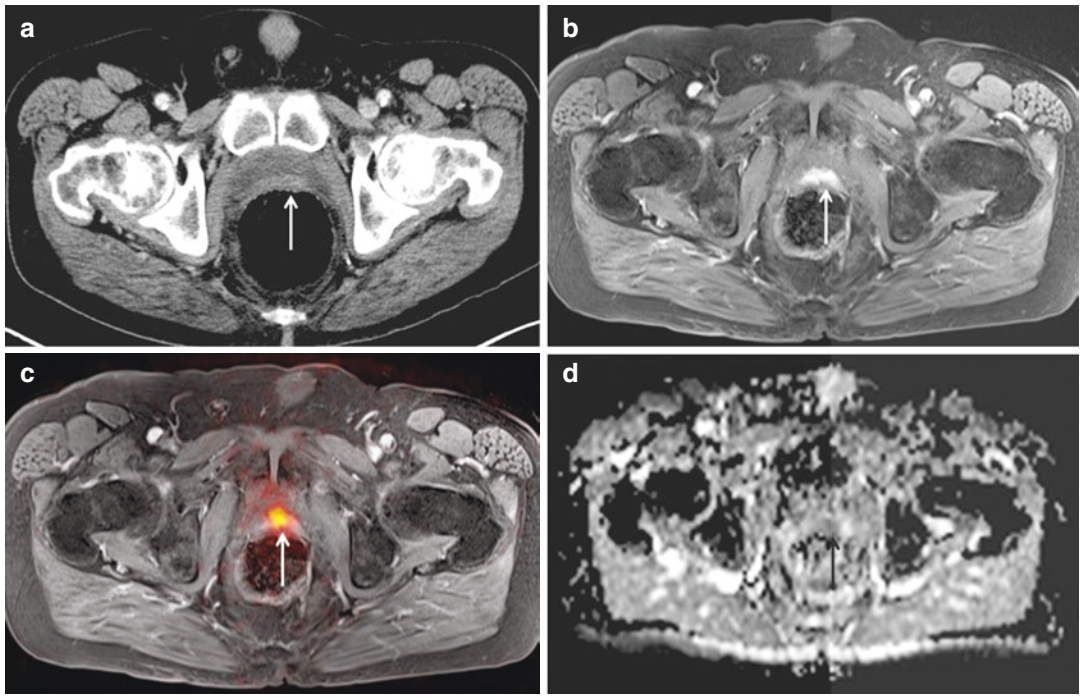

Fig. 4.2 Images from integrated ^{68}Ga PSMA-11 PET/MRI in a patient with biochemical recurrence after radical prostatectomy. PET/MRI identifies a soft-tissue lesion between the rectal and bladder wall diagnostic for local recurrence after radical prostatectomy (**b**–**d**). Due to the lack of soft-tissue contrast, it was regarded as part of the urinary bladder in PET/CT (**a**). Contrast-enhanced MRI demonstrates a clear soft-tissue mass (**b**) with ^{68}Ga PSMA-11 uptake (**c**) and a corresponding diffusion restriction (**d**)

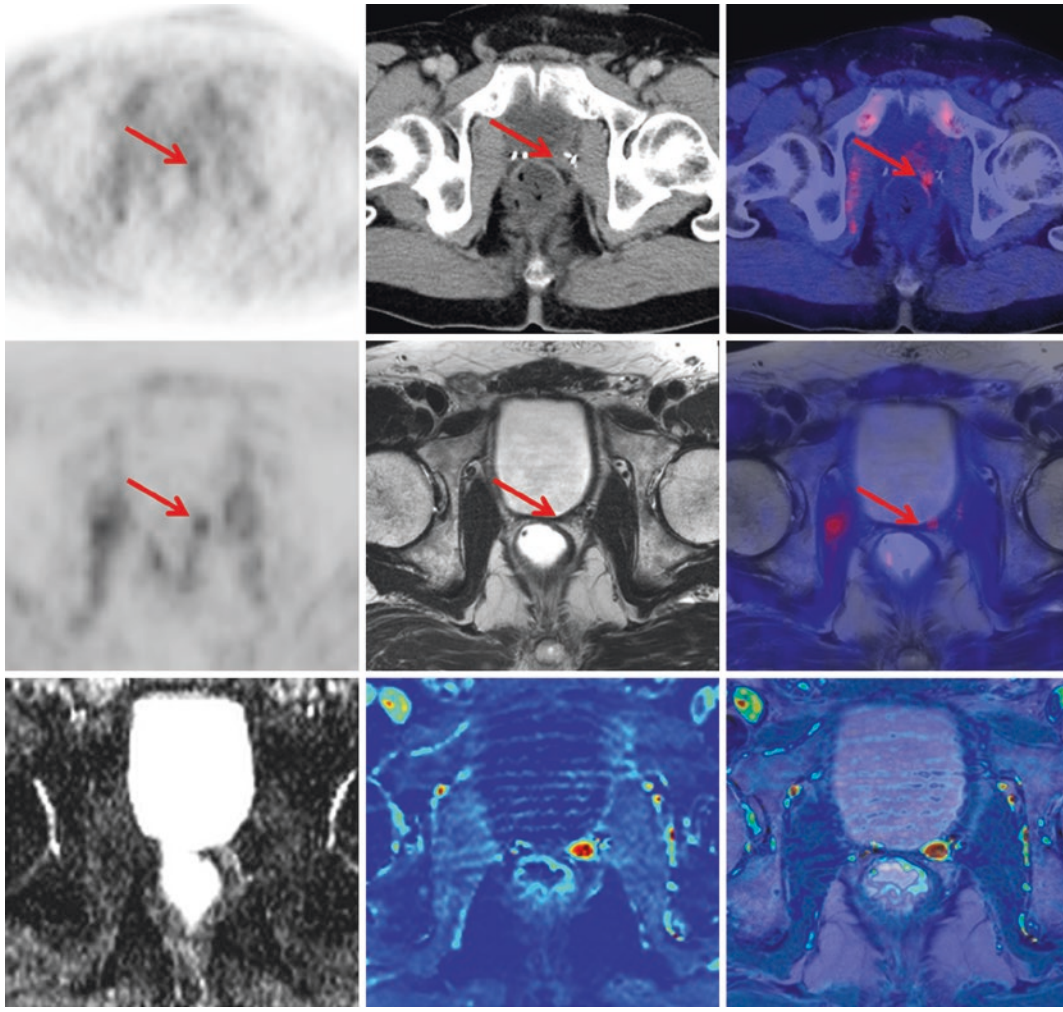

Fig. 4.3 ^{11}C-Choline PET/CT and PET/MR of a 79y/o patient with biochemical recurrence (PSA 1.7 ng/ml) after radical prostatectomy (*upper row*). PET/CT showed a faint choline uptake adjacent to the bladder on the left side which raised the suspicion for local recurrence but was judged as being unclear. PET/MR images demonstrated tracer uptake in a tiny tissue nodule (*middle row*). Additional information from the functional MR sequences showed a diffusion restriction in the ADC map (*left*, *lower row*). The iAUC60 derived from DCE (*middle*, *lower row*) and its fusion with T2w (*right*, *lower row*) demonstrated intense early contrast media influx. In conjunction with the choline uptake, the findings from functional MRI were highly indicative for a local recurrence

4.6 Outlook

Integrated PET/MRI in prostate cancer is a promising imaging modality for both primary and recurrent prostate cancer. For future key applications a clear benefit based on the combination of the molecular information from PET and excellent anatomical resolution as well as functional information from mpMRI is pertinent. Specific emerging applications include precise, imaging-

based biopsy planning in primarily biopsy-negative patients with high suspicion for prostate cancer and detection of local recurrences in patients with biochemical recurrence after primary definitive treatment.

References

Afshar-Oromieh A, Babich JW, Kratochwil C, et al. The rise of PSMA ligands for diagnosis and therapy of prostate cancer. J Nucl Med. 2016;57(Suppl 3):79S–89S.

Afshar-Oromieh A, Haberkorn U, Schlemmer HP, et al. Comparison of PET/CT and PET/MRI hybrid systems using a ^{68}Ga-labelled PSMA ligand for the diagnosis of recurrent prostate cancer: initial experience. Eur J Nucl Med Mol Imaging. 2014;41:887–97.

Afshar-Oromieh A, Malcher A, Eder M, et al. PET imaging with a [^{68}Ga]gallium-labelled PSMA ligand for the diagnosis of prostate cancer: biodistribution in humans and first evaluation of tumour lesions. Eur J Nucl Med Mol Imaging. 2013;40:486–95.

Barentsz JO, Richenberg J, Clements R, et al. European Society of Urogenital Radiology: ESUR prostate MR guidelines 2012. Eur Radiol. 2012;22:746–57.

Brierley J, Gospodarowicz MK, Wittekind C. TNM classification of malignant tumors. 8th ed. Wiley-Blackwell; 2016.

Drzezga A, Souvatzoglou M, Eiber M, et al. First clinical experience with integrated whole-body PET/MR: comparison to PET/CT in patients with oncologic diagnoses. J Nucl Med. 2012;53:845–55.

Eiber M, Maurer T, Souvatzoglou M, et al. Evaluation of hybrid ^{68}Ga-PSMA ligand PET/CT in 248 patients with biochemical recurrence after radical prostatectomy. J Nucl Med. 2015;56:668–74.

Freitag MT, Radtke JP, Afshar-Oromieh A, et al. Local recurrence of prostate cancer after radical prostatectomy is at risk to be missed in ^{68}Ga-PSMA-11-PET of PET/CT and PET/MRI: comparison with mpMRI integrated in simultaneous PET/MRI. Eur J Nucl Med Mol Imaging. 2017;44:776–87.

Fütterer JJ, Engelbrecht MR, Jager GJ, et al. Prostate cancer localization with dynamic contrast-enhanced MR imaging and proton MR spectroscopic imaging. Radiology. 2006;241:449–58.

Giesel FL, Hadaschik B, Cardinale J, et al. F-18 labelled PSMA-1007: biodistribution, radiation dosimetry and histopathological validation of tumor lesions in prostate cancer patients. Eur J Nucl Med Mol Imaging. 2017;44:678–88.

Giovacchini G, Giovannini E, Leoncini R, Riondato M, Ciarmiello A. PET and PET/CT with radiolabeled choline in prostate cancer: a critical reappraisal of 20 years of clinical studies. Eur J Nucl Med Mol Imaging. 2017;44:1751–76.

Gleason DF. Classification of prostatic carcinomas. Cancer Chemother Rep. 1966;3:125–8.

Hamoen EH, de Rooij M, Witjes JA, Barentsz JO, Rovers MM. Use of the prostate imaging reporting and data system (PI-RADS) for prostate cancer detection with multiparametric magnetic resonance imaging: a diagnostic meta-analysis. Eur Urol. 2015;67:1112–21. Review

Hara T, Kosaka N, Kishi H. Development of (18) F-fluoroethylcholine for cancer imaging with PET: synthesis, biochemistry, and prostate cancer imaging. J Nucl Med. 2002;43:187–99.

Hara T, Kosaka N, Kishi H. PET imaging of prostate cancer using carbon-11-choline. J Nucl Med. 1998;39:990–5.

Hricak H, Williams RD, Spring DB, et al. Anatomy and pathology of the male pelvis by magnetic resonance imaging. AJR Am J Roentgenol. 1983;141:1101–10.

Lee MS, Cho JY, Kim SY, et al. Diagnostic value of integrated PET/MRI for detection and localization of prostate cancer: comparative study of multiparametric MRI and PET/CT. J Magn Reson Imaging. 2017;45:597–609.

Lütje S, Cohnen J, Gomez B, et al. Integrated ^{68}Ga-HBED-CC-PSMA-PET/MRI in patients with suspected recurrent prostate cancer. Nuklearmedizin. 2017;56:73–81.

Martinez-Möller A, Eiber M, Nekolla SG, et al. Workflow and scan protocol considerations for integrated wholebody PET/MRI in oncology. J Nucl Med. 2012;53:1415–26.

Morgan VA, Kyriazi S, Ashley SE, DeSouza NM. Evaluation of the potential of diffusion-weighted imaging in prostate cancer detection. Acta Radiol. 2007;48:695–703.

Partin AW, Yoo J, Carter HB, et al. The use of prostate specific antigen, clinical stage and Gleason score to predict pathological stage in men with localized prostate cancer. J Urol. 1993;150:110–4.

Pichler WHF, Kolb A, Judenhofer MS. Positron emission tomography/magnetic resonance imaging: the next generation of multimodality imaging? Semin Nucl Med. 2008;38:199–208.

Piert M, Montgomery J, Kunju LP, et al. ^{18}F-Choline PET/MRI: the additional value of PET for MRI-guided transrectal prostate biopsies. J Nucl Med. 2016;57:1065–70.

Seith F, Gatidis S, Schmidt H, et al. Comparison of positron emission tomography quantification using magnetic resonance- and computed tomography-based attenuation correction in physiological tissues and lesions: a whole-body positron emission tomography/magnetic resonance study in 66 patients. Investig Radiol. 2016;51:66–71.

Souvatzoglou M, Eiber M, Takei T, et al. Comparison of integrated whole-body [11C] choline PET/MR with PET/CT in patients with prostate cancer. Eur J Nucl Med Mol Imaging. 2013;40:1486–99.

Sweat SD, Pacelli A, Murphy GP, Bostwick DG. Prostate-specific membrane antigen expression is greatest in

prostate adenocarcinoma and lymph node metastases. Urology. 1998;52:637–40.

Torre LA, Bray F, Siegel RL, Ferlay J, Lortet-Tieulent J, Jemal A. Global cancer statistics, 2012. CA Cancer J Clin. 2015;65:87–108.

Weinreb JC, Barentsz JO, Choyke PL, et al. PI-RADS prostate imaging - reporting and data system: 2015, version 2. Eur Urol. 2016;69:16–40.

Wetter A, Lipponer C, Nensa F, et al. Evaluation of the PET component of simultaneous ^{18}F choline PET/MRI in prostate cancer: comparison with ^{18}F choline PET/CT. Eur J Nucl Med Mol Imaging. 2014;41:79–88.

Wetter A, Lipponer C, Nensa F, et al. Simultaneous ^{18}F choline positron emission tomography/magnetic resonance imaging of the prostate: initial results. Investig Radiol. 2013;48:256–62.